Gas-particle partitioning of pesticides in the atmosphere of the North China Plain

Liping Guo[1], Shuping Shi[1], Ying Li[2], Martin Brüggemann[3], Mingyu Zhao[1], Hongyu Mu[1], Daniel M. Figueiredo[4], Junxue Wu[5], Kai Wang[1] *

[1] State Key Laboratory of Nutrient Use and Management, College of Resources and Environmental Sciences; National Academy of Agriculture Green Development; Key Laboratory of Plant-Soil Interactions of Ministry of Education, National Observation and Research Station of Agriculture Green Development (Quzhou, Hebei), China Agricultural University, Beijing 100193, PR China, [2] Key Laboratory of Industrial Ecology and Environmental Engineering (Ministry of Education), School of Environmental Science and Technology, Dalian University of Technology, Dalian 116024, China, [3] Bayer AG, Crop Science Division, R&D, Environmental Safety, Monheim, Germany, [4] Institute for Risk Assessment Sciences, Utrecht University, 3584 CM Utrecht, Netherlands, [5] Institute of Plant Protection, Beijing Academy of Agriculture and Forestry Science, Beijing 100097, China

Corresponding Author: Kai Wang, Email: kaiwang_ly@cau.edu.cn

Abstract: Pesticide residues are ubiquitous in the atmosphere in the North China Plain (NCP), with concentrations largely determined by application patterns and physicochemical parameters such as persistence and volatility. However, knowledge of gas-particle partitioning of pesticides remains limited, hindering a comprehensive understanding of their abundance, transport, and health risks. Here, we aim to elucidate the underlying mechanism of gas-particle partitioning for pesticides. In this study, 14 pairs of air and particulate matter samples were collected simultaneously in Quzhou County, the NCP. A total of 19 pesticides were observed in both gas and particulate-phases. Average pesticide concentrations in particulate phase (2025.76 ± 1048.83 pg/m³) were significantly higher than in gas phase (143.38 ± 146.31 pg/m³), accounting for 93.4% of the total atmospheric pesticide mass. Tebuconazole (662.49 ± 448.52 pg/m³), pyraclostrobin (212.01 ± 119.70 pg/m³), and carbendazim (158.68 ± 86.54 pg/m³) exhibited the highest concentrations in the particulate phase, whereas pyrimethanil (93.00 ± 79.18 pg/m³), pymetrozine (22.96 ± 21.50 pg/m³), and imidacloprid (5.78 ± 2.64 pg/m³) were predominant in the gas phase. A positive correlation between temperature and particulate-phase pesticide concentrations was found, as indicated by rising of $\log K_p$ values which is likely attributable to an interplay of pesticide physicochemical properties, ambient relative humidity, particle phase state and pesticide use patterns. Gas-particle partitioning model simulations showed absorption as the main mechanism of gas-particle partitioning, indicating atmospheric pesticides are absorbed into the interior organic film of particulate matter.

Keywords: Atmospheric pesticide, Gas-particle partitioning, Influence factor, the North China Plain

Graphic Abstract:

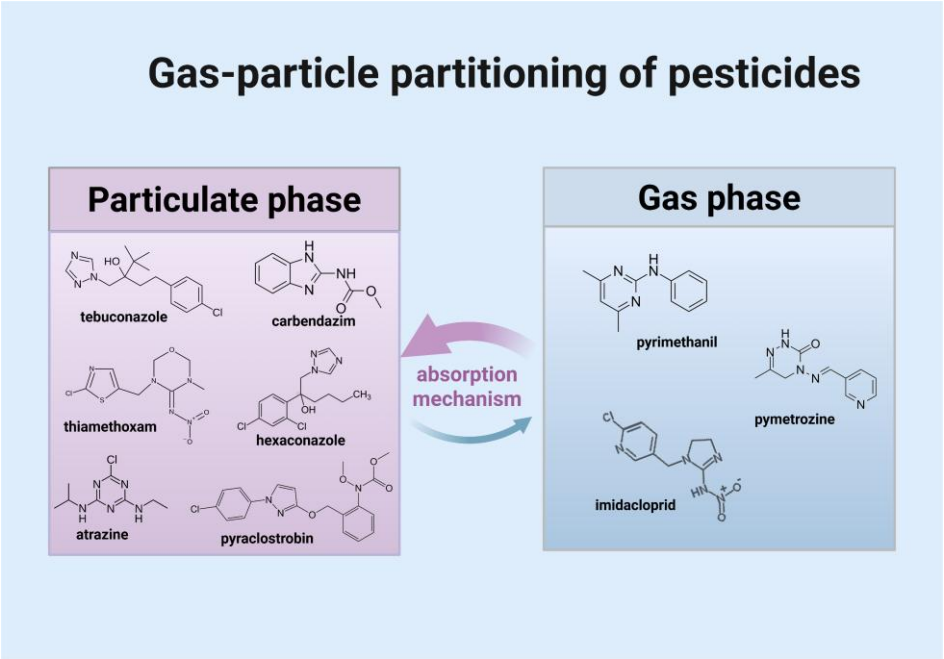

1 Introduction

Pesticides have been widely applied worldwide against pests in agriculture since dichlorodiphenyltrichloroethane (DDT) was discovered to have insecticidal properties in 1939 (Turusov et al., 2002). Pesticides play an important role in the development of agriculture by increasing the yield of agricultural products and improving their quality (Aktar et al., 2009). Pesticide usage in China reached 229,026 metric tons in 2023, accounting for around 6.14% of global pesticide use (FAO, 2025). However, the pesticide utilization rate (the proportion of the pesticide deposited on the target per unit area to the total amount of pesticide used) for the three major cereal crops (i.e., wheat, maize and rice) in China was only about 41% (China, 2021) meaning that more than half of the pesticides were not effectively absorbed by the target crops or pests and was instead lost to the environment (e.g., water, soil and atmosphere) (Tudi et al., 2022). While the fate of pesticides in soil and water has been studied extensively over the last

decades, their behavior, distribution, and degradation in the atmosphere have only recently gained increasing interest (Brüggemann et al., 2024). There are mainly three ways for pesticides to enter the atmosphere: drift, volatilization, and wind erosion. In detail this means that a portion of applied pesticides reaches the atmosphere directly during application (e.g. spray drift and vapor drift) (van den Berg et al., 1999). Later, after application, soil particles that have adsorbed pesticides may serve as a reservoir and release residues into the atmosphere through resuspension of soil particles, also referred to as wind erosion (Glotfelty et al., 1989). Furthermore, pesticides may volatilize from plants, soil, surface water, and the surfaces of old industrial sites under the influence of diffusive air-surface mass exchange (Cabrerizo et al., 2011). Atmospheric pesticides have been monitored globally. Yera and Vasconcellos analyzed concentrations of pesticides such as atrazine in the atmosphere of the São Paulo region, Brazil, ranging from 17–210 pg m^{-3} (Yera et al., 2021). In Costa Rican banana plantations, Karla et al. (2026) reported that the highest concentrations of the detected pesticides were for pyrimethanil (34.3 ng/m^3), followed by fenpropidin (9.0 ng/m^3) and terbufos (8.4 ng/m^3). Tian et al. (2021) conducted observational analysis and quantification of organochlorine pesticides in the atmosphere across nine cities in the Pearl River Delta region of China, finding that concentrations of 16 organochlorine pesticides in summer (0.33–1431 pg m^{-3}) were higher than 0.26–893 pg m^{-3} in winter. In a study on the North China Plain (NCP), ten organochlorine pesticides with concentrations ranging from 11.67 to 865.60 pg m^{-3} were observed in atmospheric $PM_{2.5}$ in a rural area of Baoding City, Hebei Province (Sun et al., 2020). Another long-term monitoring study identified chlorpyrifos, carbendazim, and atrazine as the pesticides with the highest detection rates (≥87%) in the NCP, with annual concentrations ranging from

1.71 to 16.05 pg m^{-3} (Zhao et al., 2023).

Upon entering the air, gas-particle partitioning occurs between the gas phase and particulate phase depending on the physicochemical properties of the pesticides (e.g., vapor pressure, octanol-air partition coefficient, K_{oa}), the concentrations of total suspended particulate matter (TSP) and meteorological parameters (ambient temperature and relative humidity). Among these factors, vapor pressure (V_P) is widely acknowledged as the main factor determining the effective volatilization rates. Pesticides with V_P (at 20℃) higher than 1×10^{-2} Pa are predominantly present in the gas phase, while those with V_P below 1×10^{-5} Pa can be seen as completely present in the particulate phase (Yusà et al., 2009). The conventional Junge-Pankow model attributes gas-particle partitioning to surface adsorption, whereas the absorption model assumes that chemicals dissolve into particles coated by organic films (Harner and Bidleman, 1998). Since most pesticides are semi-volatile compounds with moderate vapor pressure, they are distributed in both the gas phase and particulate phase (Bedos et al., 2002; Wang et al., 2024). Pesticides in the gas phase can be directly absorbed into the lungs and participate in the blood circulation, potentially causing adverse effects on the cardiovascular system and almost all organs (Ngo et al., 2010). The pesticides in fine particulate matter are able to penetrate deeply into the respiratory system, causing a spectrum of health hazards (Woodrow et al., 2019). These pesticides have the potential to affect various systems, such as the respiratory, circulatory, immune, and endocrine systems, and may even contribute to carcinogenesis (Kaur et al., 2019). A previous study demonstrated that the half-lives in particulate phase of difenoconazole, tetraconazole, fipronil and 8 other pesticides were longer than the estimated half-lives in the gas phase allowing them to travel longer distances (Socorro et al., 2016). Because of the

different behavior and effects of gas-phase and particulate-phase pesticides on human health and the environment, it is of great significance to study the gas-particle partitioning of atmospheric pesticides for further analysis of their health and ecotoxicological effects (Brüggemann et al., 2024).

In recent years, studies on the gas-particle partitioning of pesticides in the atmosphere mainly focused on traditional pesticides, such as organochlorine pesticides (Qiao et al., 2019). Sanli et al. studied the partitioning of organochlorine pesticides in gas phase and particulate phase at a semi-rural site in Bursa, Turkey, suggesting that the maximum annual mean gas-phase organochlorine pesticides concentration was β-hexachlorocyclohexane (β-HCH) with 176 pg/m^3 while the maximum concentration in the particulate phase was β-Endosulfan at 67 pg/m^3 (Sanlı and Tasdemir, 2020). However, due to their long lifetime in the environment, most of these pesticides are now prohibited in most countries. In contrast, modern substances exhibit significantly shorter degradation times in the environment. Still, data on gas-particle partitioning of such current-use pesticides are rarely available. Wang et al. measured the atmospheric concentrations of 36 current-use pesticides in gas phase and particulate phase samples in the Great Lakes basin and analyzed their gas-particle partitioning, suggesting that chemicals in particulate phase like metolachlor were negatively correlated with relative humidity (Wang et al., 2021). Nevertheless, there is limited evidence on the mechanism of pesticides gas-particle partitioning, which hinders our understanding of the atmospheric fate, transport and health risks of pesticides. Therefore, it is necessary to further research and understand the gas-particle partitioning of pesticides in the atmosphere.

Quzhou County is a typical agricultural county in the NCP, located in the northeastern part of

Handan City, Hebei Province (geographical coordinates: 36°35′43″–36°57′56″N, 114°50′22″–115°13′27″E; Yu et al., 2021). The total crop planting area in Hebei Province was around 8 million hectares with the pesticide usage of approximately 50,000 tons in 2023 (Hebei Provincial Bureau of Statistics, 2024). The pesticide utilization rate in Hebei Province is approximately 30%, which is lower than 50–60% observed in developed countries (Skevas et al., 2014). Given its representative agricultural setting in the NCP, Quzhou County serves as an ideal location for investigating the gas–particle partitioning of atmospheric pesticides in the NCP, thereby contributing to a more comprehensive understanding of pesticide distribution across the NCP (Feng et al., 2022). This study attempts to (1) analyze the concentrations of atmospheric pesticides in both gas and particulate phases; (2) assess the effect of meteorological factors on pesticide concentrations in the atmosphere, and (3) investigate gas-particle partitioning mechanisms using three different partitioning prediction models.

2 Materials and Methods

2.1 Air sampling

A high-volume air sampler (Sibata Scientific Technology Ltd, 080130-1203) fitted with a polyurethane foam plug (PUF, 90 mm in diameter × 50 mm in thickness) and a quartz fiber filter (QFF, 203 mm × 254 mm, pore size <0.3 μm) was used to capture pesticides in the gas phase and particulate phase (i.e. TSP), respectively. Air is first directed through the QFF for the collection of TSP, and subsequently through the PUF sampler for the collection of gaseous pesticides. Air samples were collected with a sampling period of 7 days (168 hours) at a flow rate of 150 L min^{-1} from February 17th to May 20th in 2023 at the Quzhou Experiment Station (36°78′01″N, 114°94′51″E, 40 m above sea level) in Quzhou County, the NCP. Detailed

sampling information is provided in Table S1. In total, 14 gas phase samples and 14 particulate phase samples were collected. All samples were kept at –20°C until analysis. Meteorological data (Table S2), including temperature, atmospheric pressure, precipitation, relative humidity, and wind speed, along with particulate matter (PM_{10} and $PM_{2.5}$) concentrations, were obtained from the Air Quality Monitoring Platform of Handan City (http://111.62.17.169:8083/index.html#/map/HomeTianMap) and the Quzhou Experimental Station. The mass of TSP was measured by gravimetry.

2.2 Sample treatment and instrumental analysis

The PUFs and QFFs were extracted with ultrasound-assisted extraction for 1 hour with a 100 mL mixture of hexane and dichloromethane (1:1, v-v). The extracts (80 mL) were collected in flat-bottomed flasks and then concentrated to dryness using a rotary evaporator. Next, 1 mL acetonitrile was added to each flat-bottomed flask and transferred to the centrifuge tube after sonication, with this process repeated twice. After concentration, the extracts were subsequently purified on C_{18} SPE cartridges and the columns were eluted with 5 mL of acetonitrile. All fractions were rotary evaporated to dryness and adjusted to a volume of 800 μL with acetonitrile. Finally, they were vortexed using a vortex oscillator and filtered with syringe filters and transferred to vials for detection.

Target analytes in this study included 17 fungicides, 4 herbicides, and 17 insecticides for a total of 38 compounds purchased from Alta Scientific Co., Ltd (Tianjin, China) (Table S3). The selection of these 38 pesticides is based on their high detection frequency in both gas and particulate phases, as reported in previous studies conducted in the North China Plain by Zhao

et al. (2023) and Mu et al. (2022). All solvents and chemicals used in this study were of high-performance liquid chromatography (HPLC) grade or higher. A Waters ACQUITY TQD ultra-high performance liquid chromatography system coupled with a triple-quadrupole mass spectrometer (UHPLC-MS/MS) was used to analyze the pesticides. The chromatographic and mass spectrometric conditions were consistent with Zhao et al. (Zhao et al., 2023). The UHPLC-MS/MS equipped with an ACQUITY BEH C18 column (1.7 μm, 100 × 2.1 mm i.d.). The mobile phase is increased from 5% acetonitrile (A) and 95% ultra-pure water with 0.1% formic acid (B) at 0 minutes to 95% acetonitrile over 6 minutes, then decreased to 5% A over 0.5 minutes and held for 0.5 minutes. The flow rate was 0.2 mL min^{-1} and 2 μL of individual sample was injected. The column temperature was set at 40°C. The mass spectrometer was operated in multiple reaction monitoring (MRM) mode. The calculation method for pesticide mass concentration in ambient air is provided in the Supporting Information (Text S1).

2.3 Quality assurance and quality control

To evaluate the accuracy and reliability of the data, laboratory blanks were analyzed following the same procedure as the samples, and the measured concentrations of the laboratory blank samples were very low, indicating minimal contamination during processing. The reproducibility of the spiked blanks was acceptable, yielding recoveries ranging from 45.10% ± 3.36% to 105.3% ± 3.29% for gas phase and 45.40% ± 2.64% to 122.50% ± 12.51% for particulate phase. Except for etoxazole in the gas phase (45.1%) and cycloxaprid and thiophanate-methyl in the particulate phase (both 45.4%), most pesticides showed good recovery extracted by dichloromethane and hexane. The average recoveries for 38 pesticides was 74.0±22.5% in the particulate phase and 73.5±16.8% in the gas phase. All concentration

data of this study is not adjusted using the recoveries. The limit of detection (LOD) was estimated as the quantity of analyte with a signal to noise ratio of 3:1, ranging from 0.01 pg/m^3 to 9.32 pg/m^3 for gas phase samples and from 2.22 × 10^{-4} pg/m^3 to 5.89 pg/m^3 for particulate phase samples (Table S4).

2.4 Gas-particle partitioning models

Partitioning of pesticides between the gas phase and particulate phase is often described using the gas-particle partitioning coefficient (K_P, m^3/μg) which defined by Harner and Bidleman(Harner and Bidleman, 1998):

$$K_p = \frac{C_p}{C_g \times C_{TSP}} \quad (1)$$

Where C_p and C_g are the concentrations of the pesticides (μg/m^3) in the particulate phase and gas phase, respectively and C_{TSP} is the concentration of the TSP in the air (μg/m^3).

The measured particle-bound fraction (φ_m) can be calculated by the equation(2):

$$\varphi_m = \frac{C_p}{C_p + C_g} \quad (2)$$

The gas-particle partitioning of soluble organic pollutants in the atmosphere is influenced by processes such as adsorption, absorption, as well as the removal of particulate matter through dry and wet deposition. To examine the dominant partitioning mechanisms, we tested three conceptual models, each representing a distinct hypothesis, by simulating relevant gas-particle partitioning parameters. For this purpose, we applied three established models that are widely used to simulate this process, namely the Junge-Pankow (J-P) adsorption model (Pankow, 1987; Iakovides et al., 2022), Harner-Bidleman (H-B) Koa absorption model (Iakovides et al., 2022;

196 Harner and Bidleman, 1998; He and Balasubramanian, 2009), and L-M-Y model (Li et al.,
197 2015).

198 The Junge-Pankow (J-P) adsorptive model assumes that the organic matter is adsorbed onto
199 aerosol surface and relates the predicted particle-bound fraction (φ_p) to the aerosol surface area
200 per air volume unit and the saturation vapor pressure of supercooled liquid (P_L^0, Pa) values
201 (Pankow, 1987). The φ_p can be calculated by the equation (3):

202 $$\varphi_p = \frac{c\theta}{c\theta + P_L^0} \quad (3)$$

203 Where φ is the fraction of organic matter concentration that is adsorbed onto the aerosol surface.
204 The parameter c is a constant with an empirical value of 17.2 Pa/cm. θ represents the
205 contaminated aerosol surface area per unit air volume (cm^2/cm^3) with a series of representative
206 values (1.0×10^{-7} cm^2/cm^3 for remote areas, 1.0×10^{-6} cm^2/cm^3 for rural areas, and 1.1×10^{-5}
207 cm^2/cm^3 for urban areas). P_L^0 is subcooled liquid vapor pressure calculated according to the
208 MPBPVP module in the Estimation Program Interface (EPI) suite (EPIWEB-4.1) of the U.S.
209 Environmental Protection Agency (U.S.EPA) using the mean temperature (K) during each
210 sampling period, for the pesticides atrazine, carbendazim, difenoconazole, prochloraz,
211 tebuconazole, hexaconazole, propiconazole, pyrimethanil, and omethoate, the P_L^0 values at
212 25°C were used as substitutes, since values at the actual temperature were unavailable in this
213 module (Lohmann et al., 2004). $LogP_L^0$ values for the studied pesticides are presented in Table
214 S5.

215 The Harner-Bidleman (H-B) K_{oa} absorption model predicts K_P as a function of K_{oa} and the
216 fraction of organic matter in the aerosols (f_{om}), assuming that the organic matter is absorbed

into a liquid-like organic film in the particulate matter under the influence of the absorption force, solubility and particle size (Harner and Bidleman, 1998; He and Balasubramanian, 2009):

$$\mathrm{Log}\, K_P = \log K_{oa} + \log f_{om} - 11.91 \quad (4)$$

Here, f_{om} denotes the fraction of organic matter in aerosols. Four f_{om} values (5%, 10%, 20% and 30%) were adopted following Jiang et al. (2020), and this range is highly consistent with the measured organic matter fraction of 9% to 41% for aerosols reported by Iakovides et al. (2022). This strong consistency also enhances the credibility of our simulation results. K_{oa} was calculated according to the method in KOAWIN module of the EPI suite of the U.S.EPA and the equation is as follows (Baskaran et al., 2021):

$$K_{oa} = \frac{K_{OW} \cdot RT}{HLC} \quad (5)$$

where the Kow is the octanol-water partition coefficient, with the value at 25°C acquired from the KOWWIN module in the EPI suite (EPIWEB-4.1) of the U.S.EPA. $\mathrm{LogK_{oa}}$ values for the studied pesticides are presented in Table S6. R is the ideal gas constant (Pa mol/K/m^3) with a value of 8.314. T is the mean temperature during each sampling period (K). HLC is Henry's law constant calculated according to the equation acquired from the HENRYWIN module in the EPI suite (EPIWEB-4.1) of the U.S. EPA:

$$lnHLC = A_n - B_n/T \quad (6)$$

where T is the mean temperature (K) during each sampling period. The A_n and B_n of each pesticide are different and the specific values were obtained in the HENRYWIN module.

Additionally, the φ_p can be predicted by:

$$\varphi_P = 1/\left\{1 + \left[\frac{1}{(10^{-11.9} \cdot f_{om} \cdot K_{oa}) \cdot TSP}\right]\right\} \quad (7)$$

The TSP values for each sampling period were used in this study and the typical values (5%, 10%, 20% and 30%) of f_{om} were also inserted.

The L-M-Y model was a steady-state model established by Li et al. in 2015, which considered the influences of dry and wet depositions of particles and introduced into a non-equilibrium parameter caused by dry and wet depositions, logα (McEachran Andrew et al., 2015). And the $\log K_{P\text{-}L\text{-}M\text{-}Y}$ and $\varphi_{L\text{-}M\text{-}Y}$ can be predicted according to the equations (8) and (9) as follows:

$$\log K_{P-L-M-Y} = \mathrm{Log}\, K_{p-H-B} + \log \alpha \quad (8)$$

$$\varphi_{L-M-Y} = \frac{K_{p-H-B} \cdot \alpha \cdot TSP}{1 + K_{p-H-B} \cdot \alpha \cdot TSP} \quad (9)$$

The Log $K_{P\text{-}H\text{-}B}$ can be calculated by equation (4) and the logα can be calculated by

$$\mathrm{Log}\, \alpha = -Log\left[1 + \left(\frac{2.09 \times 10^{-10} f_{om} K_{oa}}{C}\right)\right] \quad (10)$$

The values of f_{om} and the empirical constant C relative to prevailing wind were cited from previous studies(f_{om} = 5%, 10%, 20% and 30%, C = 5) in the above model (Iakovides et al., 2022).

Calculation of RMSE: RMSE for each φ_p of the pesticides detected in the gas phase and the particulate phase at the same time was calculated to statistically evaluate each partitioning model and the lower the RMSE value is, the closer is the φ_p to φ_m, indicating that the model has a better prediction of the gas-particle partitioning of the pesticides in the studied area. The RMSE can be calculated according to the equation as follows:

$$RMSE = \sqrt{\frac{\sum_{i=1}^{n} (\varphi_{mi} - \varphi_{pi})^2}{N}} \quad (11)$$

Where φ_{mi} is the measured particle fraction of each pesticide, φ_{pi} is the particle fraction predicted by each model, and N is the sample size.

3 Results and discussion

3.1 Detection frequency of pesticides in ambient air

A total of 33 pesticides was observed in the gas phase and particulate phase samples of Quzhou County during the sampling period from February 2023 to May 2023, including 17 fungicides, 12 insecticides, and 4 herbicides. The detection frequencies of these pesticides varied from 7.14 % (thiacloprid) to 100 % (acetamiprid). The detection frequencies for all quantified pesticides are given in Table S7. Twenty individual pesticides were detected at least once in both gas and particle-phase samples, with acetamiprid, imidacloprid, difenoconazole, pymetrozine, and tebuconazole detected in > 50% samples. Notably, fipronil, a pyrazole insecticide banned in agricultural production in China since 2009 (Ministry of Agriculture and Rural Affairs of the People's Republic of China, 2009), was detected in particulate phase samples on March 31st for the first time and continued to be detected in subsequent particulate phase samples until the end of sampling on May 20th, which might be due to the use of fipronil as sanitary or seed coating agent of partial dryland crop in the vicinity of the sampling site, as well as its application in controlling household pests (Cui et al., 2016).

Compared with the detection frequencies of pesticides in gas phase (64.29-85.71%), the detection frequencies in particulate phase were relatively high (71.43-92.86%). The pesticides of clothianidin, chlorobenzuron, dimethomorph, fipronil, propamocarb, thiophanate-methyl, tribenuron-methyl, triadimenol, kresoxim-methyl, azoxystrobin, trifloxystrobin and

pyraclostrobin were detected only in the particulate phase.

3.2 Concentrations of pesticides in ambient air

In total 33 pesticides were observed with the applied UHPLC-MS/MS method, including 12 insecticides, 4 herbicides and 17 fungicides (Figure 1). The average concentrations of pesticide in particulate phase (2025.76 ± 1048.83 pg/m³) were significantly higher than 143.38 ±146.31 pg/m³ in gas phase), constituting 93.4% of the total atmospheric pesticide mass. In the particulate phase, the mean concentration of tebuconazole (a broad-spectrum triazole fungicide) in the 14 QFF samples was the highest with a value of 662.49 pg/m^3, and the mean concentration of thiophanate-methyl (a thioureas fungicide) was the lowest with a value of 0.015 pg/m^3. Among the gas-phase samples, pyrimethanil (an aminopyrimidine fungicide) showed the highest mean concentration at 93.00 μg/m³ across the 14 PUF samples, attributable to its high vapor pressure. In contrast, fenbuconazole (a triazole fungicide) with low vapor pressure had the lowest mean concentration of only 0.05 pg/m³. Research has found that the pesticides in atmospheric aerosol particles are very persistent because the particles shield the absorbed compounds from degradation by OH radicals (Socorro et al., 2016). In addition, atrazine, omethoate and pyrimethanil were detected in samples taken around April 14th and the samples taken later in the gas phase, probably owing to the application or the fact that with the temperature raised, there was re-volatilization of this pesticide from contaminated terrestrial surfaces (Gungormus et al., 2021). Moreover, the pesticide physicochemical properties, their environmental persistence and the pesticide application technique used may also influence the atmospheric concentrations of the pesticides (Degrendele et al., 2016). Detailed average concentration for individual pesticides in the 14 gas-phase and 14 particulate-phase samples

collected during the sampling period from February 2023 to May 2023 are given in Table S8.

Neonicotinoid insecticides (NEOs) stand as the most extensively applied pesticides across agriculture, boasting versatile applications such as seed dressing, spraying, and soil application (Zhou et al., 2020). The average concentration of NEOs including acetamiprid, clothianidin, imidacloprid, thiamethoxam and thiacloprid in atmosphere was 241.18 pg/m^3, while it was 232.03 pg/m^3 for particulate phase and 9.15 pg/m^3 for gas phase in our study. This is at the same level as the gaseous pesticides reported by Zhao et al. (2023) from their year-round monitoring in Quzhou County, the NCP (0.6–26 pg/m^3). In comparison, the average concentration of NEOs in the particulate phase observed in this study was substantially higher than that associated with $PM_{2.5}$ in an urban area of Beijing, China (35.8 pg/m^3, March and October) and nearly three times greater than the $PM_{2.5}$-bound concentration reported for a rural area of Zhengzhou City, China (80.9 pg/m^3, March and October 2019) a conventional agricultural region, as reported by Zhou et al. (Zhou et al., 2020). Meanwhile. the concentration of individual NEOs for particulate phase (90.42 pg/m^3, 20.63 pg/m^3, 91.82 pg/m^3 and 28.71 pg/m^3 for imidacloprid, acetamiprid, thiamethoxam and clothianidin, respectively) in our study was higher than that in the rural area of Zhengzhou City, China (48.00 pg/m^3, 17.70 pg/m^3, 7.20 pg/m^3 and 7.95 pg/m^3, respectively, March and October 2019), probably due to that pesticides observed in our study were in the TSP samples (including particles with all sizes), whereas the particulate samples in the rural areas of Zhengzhou City, China were the $PM_{2.5}$ fraction. In a study on the risk assessment of airborne agricultural pesticide exposure near fields in the grain-growing area of Liaocheng City, China, Hu et al. (2024) reported concentrations of acetaminprid, atrazine, imidacloprid, and nicosulfuron detected during the sampling period from March to October 2018. The measured

concentrations were 4.88 × 10^5 pg/m^3, 2.17 × 10^3 pg/m^3, 4.11 × 10^4 pg/m^3, and 3.46 × 10^4 pg/m^3, respectively. The mean concentration of the above pesticides in our study (21.66 pg/m^3, 114.72 pg/m^3, 96.19 pg/m^3 and 2.17 pg/m^3) was lower than that of the research in Liaocheng City, China, which may be related to the low pesticide application near the sampling site during the sampling period in this study.

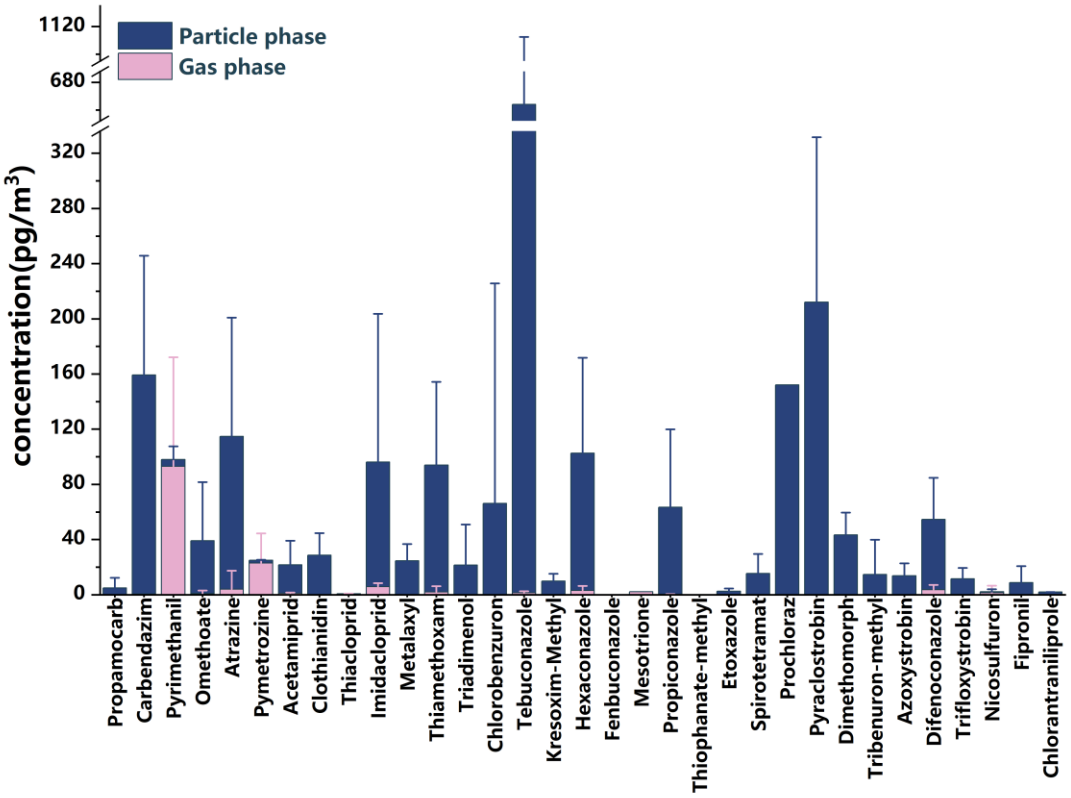

Figure 1. The average concentration of individual pesticide in the 14 gas phase (light green) and 14 particulate phase (dark green) samples collected during the sampling period from February 2023 to May 2023. In total 33 pesticides were observed with the applied UHPLC-MS/MS method.

3.3 Temporal variation of pesticide concentration

The concentrations of four typical fungicides (i.e., tebuconazole, prochloraz, pyraclostrobin, and propiconazole) and the insecticide imidacloprid increased in the particulate phase in mid-April and early May (Figure 2, Figures S1-S2). In the gas phase, imidacloprid, atrazine, tebuconazole, and propiconazole showed a similar trend but at lower concentrations than in the particulate phase, except for pyrimethanil, which had a higher concentration in the gas phase on April 29th. The concentration of hexaconazole in the gas phase and the particulate phase had a similar trend over time (Figures S1–S2). This trend aligns with the application timing during the booting and heading stages of wheat (early April to mid-May), with peak concentrations coinciding with pesticide application. In addition, the concentrations of hexaconazole and imidacloprid in the gas phase were higher than particulate phase before April (the month of wheat booting stage), this might be caused by the volatilization of pesticides from the soil to the atmosphere. Although the temporal distribution patterns of other pesticides in the gas and particulate phases do not exhibit a high degree of consistency, a notable increase in particulate-phase concentrations was observed from April to mid–May (Figures S1–S2). Notably, this period corresponds to the key pre-harvest window for pest and disease control in wheat, which coincides with the booting and heading stages (early April to mid–May).These findings suggest that pesticide applications near the sampling site resulted in emissions into the atmosphere and subsequent association with atmospheric particulate matter. Moreover, the temporal pattern indicates that local sources (e.g., pesticides application in the local fields) dominated atmospheric pesticide concentrations.

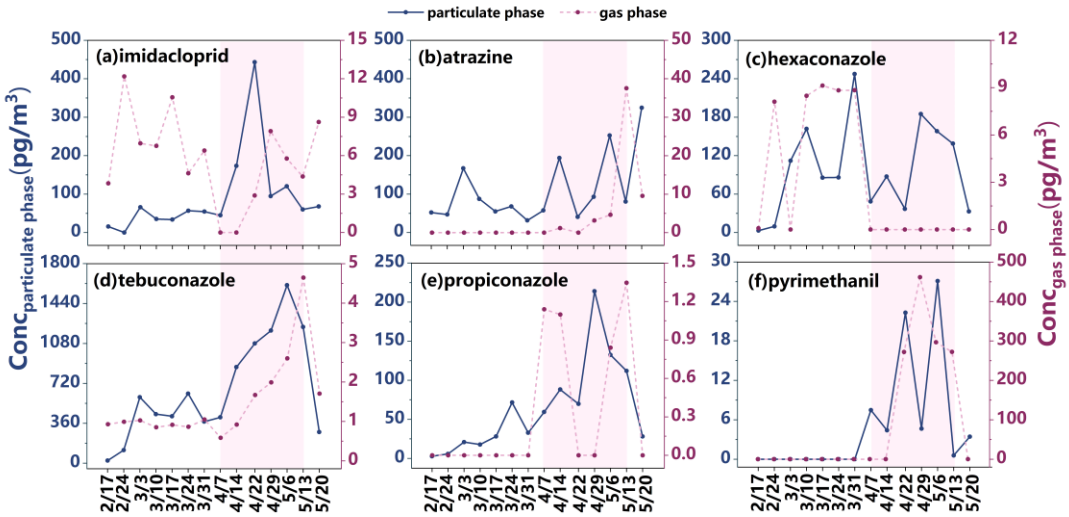

Figure 2. The concentration trend of different pesticides with sampling dates in particulate phase (full line) and gas phase (dotted line) from February 2023 to May 2023. (a) imidacloprid. (b) atrazine. (c) hexaconazole. (d) tebuconazole. (e) propiconazole. (f) pyrimethanil. The left coordinate axis represents the concentration of pesticide in particulate phase and the right coordinate axis represents the concentration in gas phase. In the figure, the purple shadow denotes the wheat growth stages from booting to heading.

3.4 Effect of meteorology on pesticide concentrations in both particulate and gas phase

To elucidate major factors influencing pesticide distribution between the particulate and gas phases, we used a Pearson correlation matrix to visualize the relationships among total pesticide concentrations in both phases, meteorological parameters, and particulate matter (PM_{10}, $PM_{2.5}$ and TSP) concentrations (Figure 3). A positive correlation with a correlation coefficient of 0.66 ($p < 0.01$) between the particulate and gas-phase pesticide concentrations was observed, indicating that pesticides in both particulate and gas phase share common sources. A significant negative correlation was observed between the pesticide concentration in particulate + gas phase and reciprocal temperature ($r = –0.71$, $p < 0.01$). In other words, rising temperature leads

to an increase of the total concentration of pesticides in the atmosphere, including those in both gaseous and particulate phases. It can be explained by that more pesticides volatilized from the soil to the atmosphere with high temperature, which aligns with the finding by Iakovides et al. (2022). Figure 3 shows a lack of significant correlation between pesticide concentrations (both particulate and gaseous) and wind speed, suggesting that the pesticide concentration in the atmosphere in this study was dominated by local emission sources rather than long-distance sources by wind. In addition, a significant negative correlation was observed between reciprocal temperature and pesticide concentration in the particulate phase ($r = –0.72$, $p < 0.01$), whereas no statistically significant correlation was found with the concentration in the gas phase. Thus, increasing temperatures were connected to an enrichment of pesticides in the particle phase. This finding is somewhat unexpected, as increased temperatures typically promotes the phase transition of semivolatile organic compounds from the particulate to the gaseous phase. This phenomenon deserves attention and requires further analysis of its underlying causes. Wang et al. (2024) identified temperature as the primary factor influencing the gas-particle partitioning of polycyclic aromatic hydrocarbons (PAHs). This provides a possible explanation, but further verification is needed in our study. Atmospheric pesticide concentrations showed no significant correlations with precipitation, relative humidity, or wind speed. Negative correlations ($r = –0.54$ to $–0.32$) were observed between pesticide concentrations (in both particulate and gas phases) and levels of PM_{10} or $PM_{2.5}$.

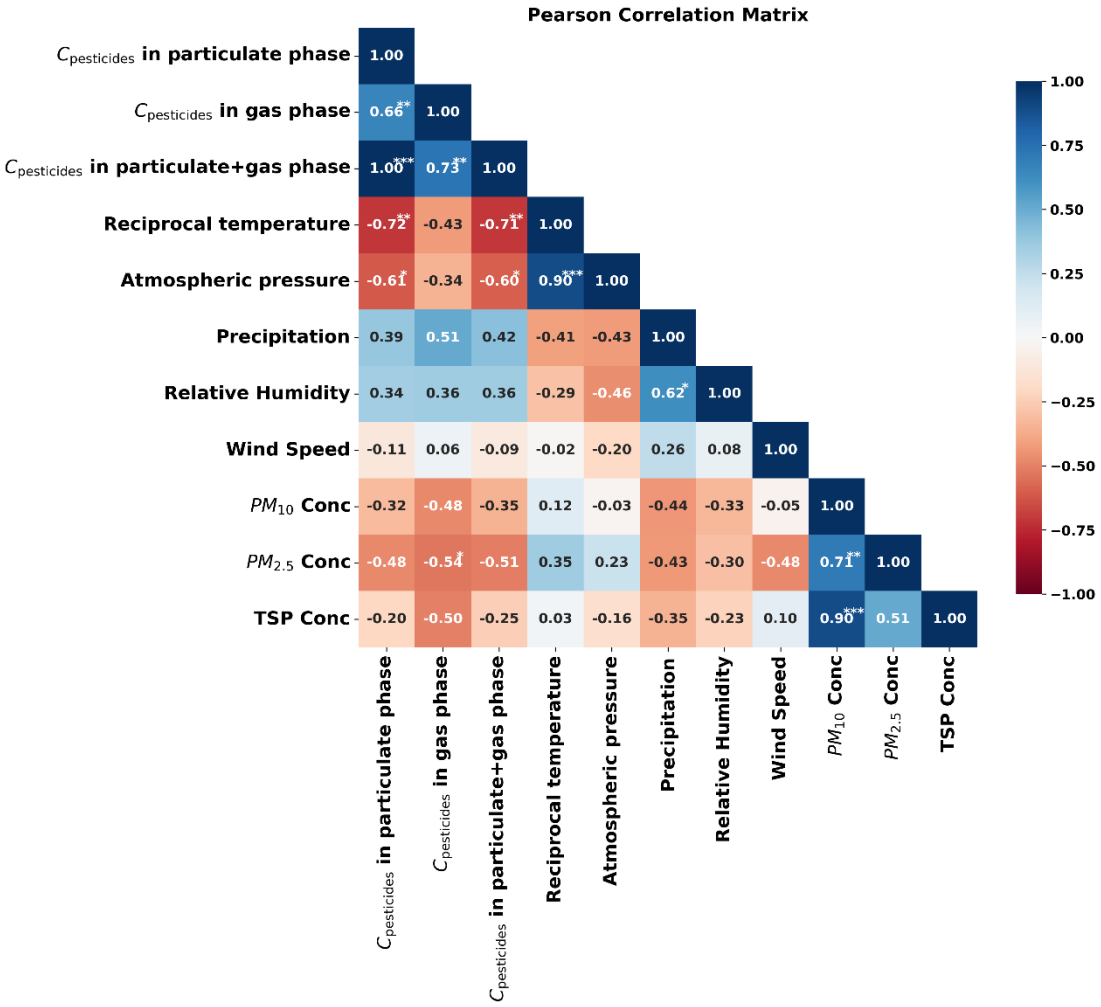

Figure 3. Pearson correlation matrix of pesticide concentrations in particulate phase, gas phases and particulate+gas phase with meteorological parameters and particulate matter (PM_{10}, $PM_{2.5}$ and TSP) concentrations. The values in the cells represent Pearson correlation coefficients (r). Asterisks indicate statistical significance: *p < 0.05, **p < 0.01, and ***p < 0.001.

To further investigate the influence of temperature, we performed a correlation analysis between temperature and the log K_P values of pesticides meeting the criterion of having more than five valid data points (i.e., acetamiprid, imidacloprid, difenoconazole, pymetrozine, tebuconazole, and hexaconazole), as shown in Figure 4. The log K_P values of all six pesticides increased with rising temperature. Notably, this correlation was statistically significant for

acetamiprid, difenoconazole, and pymetrozine, indicating that higher temperatures were associated to their partitioning into the particulate phase. This pattern was mirrored by the relationship between temperature and the ratio of particulate-phase to gaseous-phase concentration (C_p/C_g) (Figure S4). A study by Zhu et al. in Harbin City, China reported negative correlations between temperature and log K_P for most 4–5 ring PAHs, whereas positive correlations were observed for the 3-ring PAHs (acenaphthylene and acenaphthene) (Zhu et al., 2021). This contrast highlights the pivotal role of physicochemical properties, which can lead to completely opposing temperature dependencies for log K_P. Ulteriorly, the positive correlation between temperature and the particulate-phase fraction of pesticides, shown in Figure S5, may be compounded by concurrent increases in relative humidity. Specifically, when temperatures exceed 290 K, relative humidity is consistently observed to be above 52%. Under these conditions, elevated humidity can induce a phase transition in particulate matter, decreasing its viscosity and transforming it into a liquid-like state (Li and Shiraiwa, 2019). This physical change subsequently strengthens the particle's capacity to absorb and retain pesticides. Furthermore, agricultural activities (e.g., soil tillage) subsequent to pesticide application in spring can accelerate the release of fine soil particles containing pesticides to the atmosphere by wind erosion, resulting in the increase of pesticides in the particulate phase (Mayer et al., 2024).

Therefore, as temperature increased, elevated concentrations of pesticides in the particulate phase were observed in this study, accompanied by a rise in log K_p values. This indicates an increase in the C_p/C_g ratio with temperature. Pearson correlation and linear regression analyses suggest that this trend is likely not governed by a single factor, but rather results from multiple

interacting drivers, including the physicochemical properties of pesticides, increasing relative humidity, the transition of particles to a liquid-like phase, and heightened pesticide application.

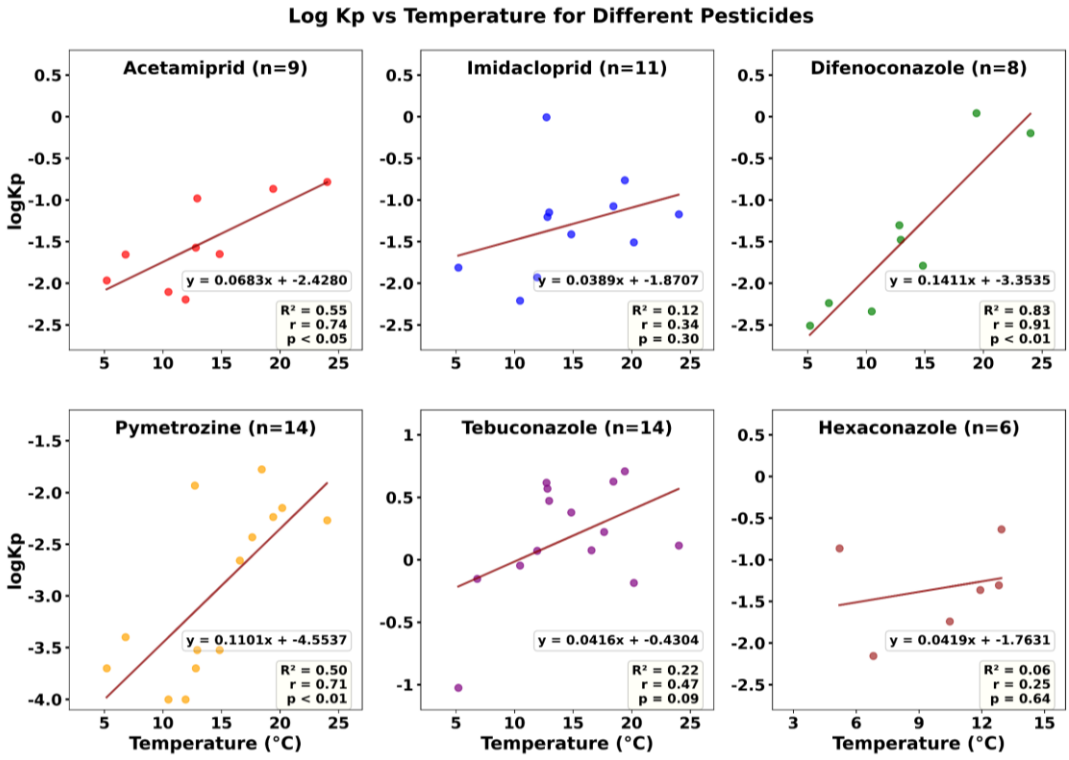

Figure 4 The correlation between log K_P for pesticides and temperature. The "n" in the figure represents the number of valid data points for each type of pesticide in the logK_P measurement. Pearson correlation analysis was conducted between log K_P and temperature for pesticides with more than five valid data points. R^2 represents the coefficient of determination for Pearson correlation, r represents the correlation coefficient, and p represents the significance level.

3.5 Gas-Particle partitioning

In our study, the gas-particle partitioning coefficient K_P calculated by equation (1) are summarized in Table S9. In general, tebuconazole exhibited the highest partition coefficient (K_p, 0.09–5.1 m^3/pg) across all sampling periods, indicating a greater tendency for distribution in the particulate phase, likely due to its low saturation vapor pressure of supercooled liquid (P^o_L). The K_P of pymetrozine was markedly low from the February 17th to March 31st in 2023

437 and increased significantly from April[7th] to May[20th] in 2023, indicating an approximate tenfold
438 variation. This phenomenon may be attributed to the progressive partitioning of pymetrozine
439 into the particulate phase over time. Alternatively, the increased application of pesticides during
440 the booting and heading stages of wheat could also be a contributing factor. During these stages,
441 the elevated pesticide usage may lead to emission into the atmosphere, where the pesticides
442 subsequently bind to atmospheric particulate matter. Other pesticides, including acetamiprid,
443 imidacloprid and difenoconazole, also showed the same pattern of K_P. In addition to pesticide
444 application patterns, an extended sampling duration may lead to the redistribution or
445 degradation of pesticides during the sampling process itself, which could consequently affect
446 the measured partition coefficient (K_p) values. However, a recent study by Karla et al. (2026)
447 showed that the pesticide concentrations in PUF samplers collected in one week were consistent
448 with that in three weeks, indicating no significant degradation or diffusion of pesticides in PUF
449 samplers within three weeks. Therefore, the impact of redistribution and/or degradation process
450 of pesticides during one-week sampling period on the gas-particle partitioning of pesticides is
451 very limited.

452 Measured particle-bound fraction φ of 18 pesticides detected in the gas phase and the particulate
453 phase were plotted against the corresponding P_L^0 and compared with theoretical curves at given
454 θ representing remote, rural and urban areas. Overall, the results presented in Figure 5 show
455 that most φ values ranged from 0.7 to 1, suggesting a potential underestimation of φ and
456 highlighting the limitations of the adsorptive model in accurately simulating φ for most
457 pesticides. This also implies the possible involvement of additional absorption mechanisms
458 beyond surface adsorption.

While gas-particle partitioning models mostly assume thermodynamic equilibrium, kinetic effects that lead to non-equilibrium states are not captured by the models. Under field conditions, several factors, such as pesticide source and transport (e.g., drift, volatilization after application and wind erosion of contaminated soil), the interval between application and sampling, the distance between application and sampling sites, and environmental conditions, might significantly affect gas-particle partitioning (Scheyer et al., 2008). Therefore, the underestimation may be due to pesticides, deposited on soil surfaces, that were resuspended into the atmosphere by wind erosion, and sampled before gas-particle partitioning reached an equilibrium state.

Furthermore, some uncertainties associated with sampling and analysis methods could also contribute to differences between theoretical and experimental data. For example, about half of the P_L^0 values used in predictive models were calculated at 25°C by the U.S.EPA's EPI suite (v.4.1). In this study, however, samples were collected in winter and spring at temperatures considerably lower than 25°C (i.e., 0.5–22°C). Considering that P_L^0 of pesticides decreases with lower temperatures, partitioning into the particulate phase is favored. Consequently, there were more pesticides distributing in the particulate phase under actual conditions, which caused higher particle fraction (φ_m) of each pesticide and underestimation of the model. In addition, due to the lack of adequate field measurements, c and θ values were estimated from other studies. Since the constant c varies for different groups of compounds, the value of 17.2 Pa/cm may not always be appropriate for each pesticide. The value of θ was also affected by the heterogeneous composition of atmospheric aerosols (contents of organic and elemental carbon), introducing uncertainty into model predictions. Additionally, the results further confirmed that

the surface area of particulate matter in China may differ from that in Western Europe and the United States (Fleagle, 1963; Harner and Bidleman, 1998). The air pollution in China is caused by the production of highly primary emissions and secondary aerosols, while the Great Smog of London and Los Angeles mainly resulted from coal combustion and photochemical oxidation of vehicle emissions, respectively (An et al., 2019). Therefore, the actual contaminated TSP surface area per unit of air volume in Quzhou County should be greater than 1.1×10^{-5} cm^2/cm^3, which was used in this model for the urban area.

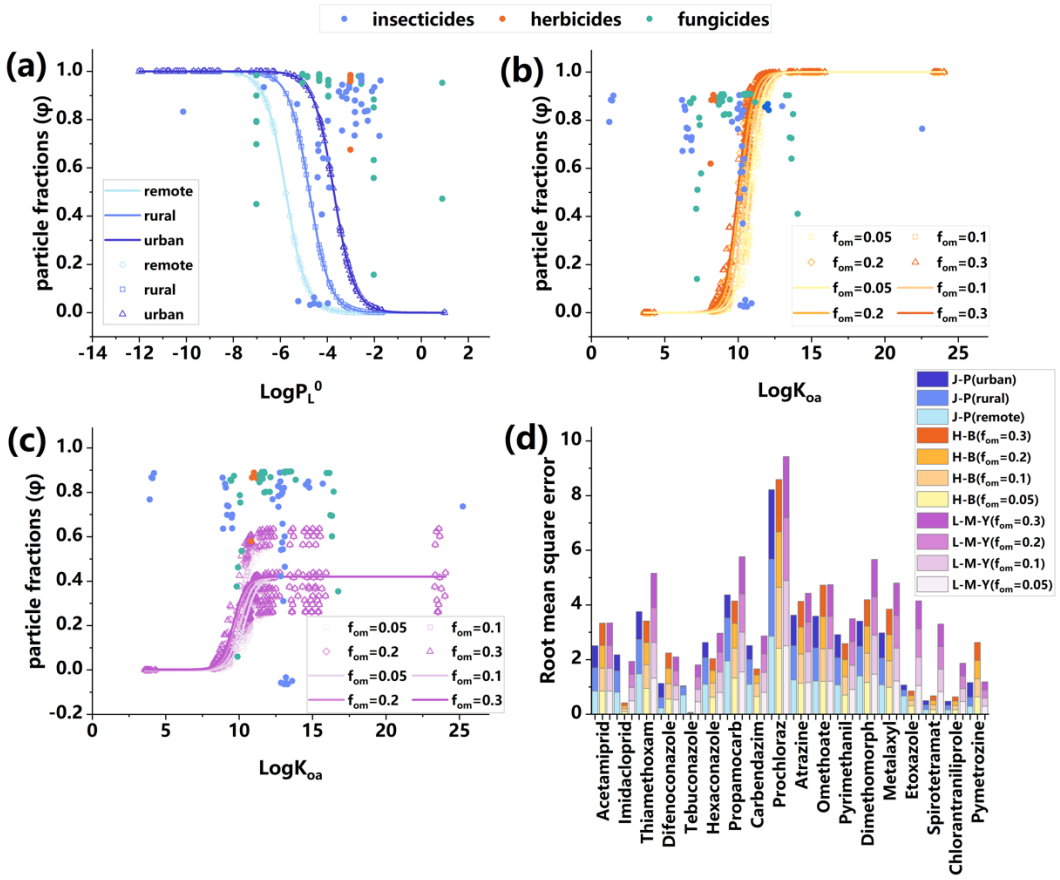

Figure 5. Measured vs. predicted particle fractions (φ) by applying J-P model (a), H-B model (b) and L-M-Y model (c) for 18 major pesticides detected both in particulate phase and gas phase. (d) The root mean square error (RMSE) of the particle phase fractions of 18 pesticides predicted by the J-P model, H-B model and L-M-Y model. The empty

dots of different colors represent the predicted φ values from three models, while the solid dots correspond to the measured φ values for various pesticides (insecticides, herbicides, and fungicides) examined in this study. The curves illustrate the predicted trends of φ values (represented by empty dots). In Figure 5(a), the line colors indicate different levels of contaminated aerosol surface area per air volume unit across remote, rural, and urban areas. In Figures 5(b) and 5(c), the colors correspond to different fractions of organic matter (f_{om}) in the aerosols.

In addition to the J-P adsorption model (Figure 5a), measured φ particle fractions for 18 pesticides detected in both the particulate phase and gas phase were plotted against their corresponding $logK_{oa}$ values and compared with theoretical partitioning curves at given f_{om} values (0.05, 0.1, 0.2 and 0.3) based on the H-B absorptive model (Iakovides et al., 2022). As shown in Figure 5b, the φ values predicted by the K_{oa} absorption model exhibited greater alignment with theoretical values compared to those predicted by the J-P adsorption model. The fitting of the pesticides (atrazine, prochloraz, hexaconazole and imidacloprid) with $LogK_{oa}$ in the range of 9.98–12.10 was better, with prochloraz and hexaconazole exhibiting the most precise fitting. This indicates that, compared to the adsorption mechanism, the absorption mechanism was the main mechanism to describe the gas-particle partitioning of the pesticides, This might be related to the fact that the increase in temperature causes K_{oa} to increase (Eq 4), thereby facilitating the distribution of pesticides into the organic phase, which is consistent with the previous analysis of influencing factors.

For pesticides with $LogK_{oa}$ values less than 9.98 (omethoate, acetamiprid, propamocarb, metalaxyl and pyrimethanil), all four prediction curves were significantly underestimated. This discrepancy can be attributed to the calculation of K_{oa} values in the model based on the K_{OW} equation at 25°C, while the samples were collected in winter and spring at temperatures lower

than 25℃. Considering that the K_{oa} of pesticides increases with the decreasing temperature, this weakens the trend of the transformation into the gas phase, resulting in more pesticides distributing in the particulate phase under actual conditions, and caused higher φ values. However, for the pesticides with $LogK_{oa}$ bigger than 12.10 (difenoconazole, thiamethoxam, chlorantraniliprole and partial pymetrozine), there was overestimation in all of four curves, which may be related to the fact that the gas-particle partitioning of these pesticides did not reach the equilibrium state. Both K_{oa} and P_L^0 model observations described above imply that adsorptive and absorptive partitioning are not strong standalone predictors for the pesticides in the studied atmosphere.

Measured φ particle fractions for the 18 pesticides mentioned above were also plotted against their corresponding $logK_{oa}$ values and associated with theoretical curves at given f_{om} values (0.05, 0.1, 0.2 and 0.3) based on the L-M-Y steady-state model. As shown in Figure 5c, the L-M-Y model underestimated the distribution in the particulate phase for almost all of the pesticides, and the fitting performance of the model was inferior to that of the H-B model, indicating that the distribution of pesticides on particulate matter was closer to the equilibrium state than that of the steady state. In addition, the farther the distance from the pesticide application sites to the sampling sites, the higher the proportion of pesticides that distribute in the particulate phase (Amelia et al., 2005). Therefore, in this model, the underestimation of φ values may stem from both local sources and long-range atmospheric transport of pesticides.

To better identify the prediction outputs of the three models, the RMSE for each φ_p of the pesticides detected in the gas phase and the particulate phase at the same time was calculated. As shown in Figure 5d, for most of the pesticides, the RMSE values of the L-M-Y model were

higher than those of the other two models, indicating that the L-M-Y model had poorer predictive performance. The RMSE values of the J-P and H-B models were comparable, with the H-B model yielding lower RMSE values for 8 pesticides and the J-P model yielding lower RMSE values with 10 pesticides. Although more pesticides fitted with the J-P model achieved lower RMSE values compared to the H-B model, the mean RMSE value of the H-B model was lower than that of J-P model, suggesting slightly stronger predictive capability of the H-B model for φ values.

Additionally, the trends of the logarithm of the measured gas-particulate partition coefficient (K_{pm}) to the predicted gas-particulat partition coefficient (K_{pp}) and K_{oa} log-log relationships for the H-B model and L-M-Y model were also explored and the closer the slope derived from the fitting line to 0, the better the agreement between K_{pm} and K_{pp} and the results are shown in Figure S3. Compared to the H-B model, the slope of $LogK_{pm}$/$LogK_{pp}$ and $LogK_{oa}$ fitting line predicted by L-M-Y model was closer to 0, indicating that the L-M-Y model may have better predictive performance. However, both two models produced lower R^2, which might be due to excessive $LogK_{pm}$/$LogK_{pp}$ values for individual pesticides (pymetrozine, tebuconazole and imidacloprid). Therefore, this chapter considers the actual fitting performance of each model and the results calculated according to RMSE.

In general, the K_P of tebuconazole was the highest in each sampling period, indicating that the pesticide was more likely to be distributed in particulate phase during the sampling period, likely due to its low P^o_L. The K_P values of pymetrozine, acetamiprid, imidacloprid and difenoconazole were very low in the first half of the entire sampling period and increased in the last half of the entire sampling period, owing to the fact that more pesticides distributing into

the particulate phase as time went on or due to an increasing number of pesticides applied in the fields around sampling site. Compared with the other two models, the H-B model could better predict the gas-particle partitioning of pesticides in the atmosphere in Quzhou. The absorption mechanism was the main mechanism to describe the partitioning on particulate matter, but it was not an independent predictor, and other mechanisms were also controlling the gas-particle partitioning. In addition, the gas-particle partitioning in the atmosphere was closer to the equilibrium state rather than the steady state, but it still had not reached equilibrium state. However, field conditions may not be at equilibrium, a possible explanation is that the pollution in the study area primarily originated from local short-range emissions, as the sampling sites were located near farmland. High-intensity, close-range emissions could have established strong concentration gradients in the media surrounding the source, thereby dominating the short-term atmospheric partitioning behavior of pesticides near our sampling points and driving it rapidly toward local equilibrium. At the same time, regional atmospheric advection and long-range transport likely exerted a relatively weak influence given the spatial and temporal scales of this study. Therefore, although environmental systems are generally open and non-equilibrium on macroscopic and long-term scales, under specific localized and short-term conditions, equilibrium models may still serve as effective simulation tools.

4 Limitation

This study has the following two limitations. Firstly, we estimated the gas-particle partitioning coefficient (K_p) using four assumed fractions of organic matter (f_{om})—5%, 10%, 20%, and 30%—rather than measured organic matter content. Although the assumed range was informed by reported organic matter content in particulate matter (9–41%; Iakovides et al., 2022), these

values may still deviate from site-specific conditions. This approach could introduce uncertainty in predicting pesticide adsorption to the particulate phase. In addition, it is also important to note the limitation imposed by the sampling timeframe (March to May). Seasonal shifts can alter both pesticide usage and meteorological factors, leading to substantial differences in gas-particle partitioning across the year. Consequently, the findings may not fully represent year-round patterns. Future research should include year-round monitoring to address this temporal variation.

5 Conclusions

Utilizing UHPLC-MS/MS method and partitioning prediction models, this study focused on the gas-particle partitioning of pesticides in Quzhou County, the NCP. Our study demonstrates that pesticides were predominantly present in the particulate phase, accounting for up to 93.4 % of the total concentration in the atmosphere. The concentrations of most pesticides in the particulate phase and gas phase reach the maximum between mid-April and May suggesting that regional pesticide application patterns drive the temporal concentration trends. It was found that an increase in temperature significantly promoted the concentration of pesticides in the atmosphere. Moreover, a positive correlation between temperature and particulate-phase pesticide concentrations was observed, as indicated by rising $\log K_p$ values. This pattern is likely driven by a combination of factors, including pesticide physicochemical properties, ambient relative humidity, particle phase state and pesticide use patterns. The H-B model could better predict the gas-particle partitioning of pesticides in the atmosphere, and the absorption mechanism is the main mechanism to describe the partitioning on particulate matter. In general, this study indicates that pesticides are mainly absorbed into the internal organic films of

particulate matter in the NCP and advances the understanding of pesticide fate in the atmosphere of the NCP. To further elucidate pesticide behavior in particulate matter, future study should investigate the occurrence and transformation of pesticides across different particle size fractions, especially the fine particles.

Data Availability

The data sets generated in the current study are available at https://zenodo.org/records/17641894?preview=1&token=eyJhbGciOiJIUzUxMiJ9.eyJpZCI6ImM0ZDAwOWUwLTY4YjAtNGFmMy1iZGFiLWE4YWFjZmE4NDE1ZSIsImRhdGEiOnt9LCJyYW5kb20iOiI2ZDhhMTU4MDc1Zjg4YThjODFiZTkyZjk0ZTI5OTE2NyJ9.R1A8yqr2bWZgp_fe95aDW33pY5MJoF8vFbG8tap-dAiQk9jQJOU_fHWipa8of7cdn0GzqRHyy2-USZeDjk-5VQ (Guo et al., 2025, https://doi.org/10.5281/zenodo.17641894). Figures were made with Matplotlib version 3.8.4 (https://zenodo.org/records/10916799), available under the Matplotlib license at https://matplotlib.org/.

Supporting Information

The detailed description of calculation of the mass concentration of pesticides in ambient air (text S1); the trend of different pesticide concentrations in particulate phase with time during the sampling period from February 2023 to May 2023 (Figure S1); the trend of different pesticide concentrations in gas phase with time during the sampling period from February 2023 to May 2023 (Figure S2); the slope of $LogK_{pm}/LogK_{pp}$ and $LogK_{oa}$ fitting line predicted by L-

623 M-Y model and H-B model (Figure S3); the correlation between C_g/C_p for pesticides and
624 temperature (Figure S4); the correlation between particulate-phase pesticide concentration and
625 temperature (Figure S5); the information of the samples (Table S1); the information of the
626 meteorological data in the sampling period (Table S2); the information of standard substance
627 (Table S3); the limit of quantitation and limit of detection (Table S4); the log P_L^0 of each
628 pesticide in each sampling period (Table S5); the log K_{oa} of each pesticide in each sampling
629 period (Table S6); the detection frequency of the pesticides in gas phase and particulate phase
630 (Table S7); the concentration of the pesticides in gas phase and particulate phase (Table S8);
631 the gas-particle partition coefficients of the pesticides (Table S9).
632

633 **Author contributions**

634 Kai Wang contributed in designed the experiments and fundings for this work. Liping Guo was
635 responsible for data analysis and manuscript preparation. Shuping Shi is responsible for
636 conducting the experiment. Mingyu Zhao and Hongyu Mu provided guidance for the
637 experiment. Ying Li provided guidance on the gas-particle partitioning model part. Martin
638 Brüggemann, Daniel M. Figueiredo and Junxue Wu provided guidance on article writing.
639

640 **Competing interests**

641 The authors declare that they have no known competing financial interests or personal
642 relationships that could have appeared to influence the work reported in this paper.

643 **Acknowledgements**

The authors gratefully acknowledge the financial support from the National Natural Science Foundation of China (No. 42207125 and No. 42475124); Professor Station of China Agricultural University at Xinzhou Center for Disease Control and Prevention; Mingyu Zhao acknowledges the China Scholarship Council (No. 201913043).

Financial support

This research has been supported by the National Natural Science Foundation of China (No. 42207125 and No. 42475124), Professor Station of China Agricultural University at Xinzhou Center for Disease Control and Prevention and the China Scholarship Council (No. 201913043).

References

Aktar, M. W., D. Sengupta, and A.: Chowdhury. Impact of pesticides use in agriculture: their benefits and hazards, Interdisciplinary toxicology, 2(1), 1, http://doi.org/10.2478/v10102-009-0001-7, 2009.

Amelia, S, Clymo, Jin, Young, Shin, Britt, A, and Holmén.: Herbicide Sorption to Fine Particulate Matter Suspended Downwind of Agricultural Operations: Field and Laboratory Investigations, Environ. Sci. Technol., 39(2), 421–430, http://doi.org/10.1021/es049210s, 2005.

An, Z., R. J. Huang, R. Zhang, X. Tie, G. Li, J. Cao, W. Zhou, Z. Shi, Y. Han, and Z. Gu.: Severe haze in northern China: A synergy of anthropogenic emissions and atmospheric processes, Proceedings of the National Academy of Sciences of the United States of America, 116(18), 8657-8666, http://doi.org/10.1073/pnas.1900125116, 2019.

Barredo Yera, A. M., Vasconcellos, P. C.: Pesticides in the atmosphere of urban sites with different characteristics, Process Saf Environ, 156, 559-567, https://doi.org/10.1016/j.psep.2021.10.049, 2021.

Baskaran, S., Y. D. Lei, and F. Wania.: Reliable Prediction of the Octanol-Air Partition Ratio, Environ Toxicol Chem, 40(11), 3166-3180, http://doi.org/10.1002/etc.5201, 2021.

Bedos, C., P. Cellier, R. Calvet, and E. Barriuso.: Occurrence of pesticides in the atmosphere in France, Agronomie, 22(1), 35-49, http://doi.org/10.1051/agro:2001004, 2002.

Brüggemann, M., S. Mayer, D. Brown, A. Terry, J. Rüdiger, and T. Hoffmann.: Measuring pesticides in the atmosphere: current status, emerging trends and future perspectives, Environmental Sciences Europe, 36(1), 39, http://doi.org/10.1186/s12302-024-00870-4, 2024.

Cabrerizo, A., J. Dachs, K. C. Jones, and D. Barceló.: Soil-Air exchange controls on background atmospheric concentrations of organochlorine pesticides, Atmos. Chem. Phys., 11(24), 12799-12811, http://doi.org/10.5194/acp-11-12799-2011, 2011.

Cui, J. K., Huang, W. K., Peng, H. Lv, Y., Kong, L. A., Li, H. X., Luo, S.-J.,Wang, Y. and Peng, D. L.: Efficacy Evaluation of Seed-Coating Compounds Against Cereal Cyst Nematodes and Root Lesion Nematodes on Wheat, Plant Disease, 101(3), 428-433, http://doi.org/10.1094/PDIS-06-16-0862-RE, 2016.

Degrendele, C., K. Okonski, L. Melymuk, L. Landlova, P. Kukucka, O. Audy, J. Kohoutek, P. Cupr, and J. Klanova.: Pesticides in the atmosphere: a comparison of gas-particle partitioning and particle size distribution of legacy and current-use pesticides, Atmos. Chem. Phys., 16(3), 1531-1544, http://doi.org/10.5194/acp-16-1531-2016, 2016.

FAO.: Pesticides use and trade – 1990–2023. FAOSTAT Analytical Briefs, No. 109. Rome. , http://doi.org/https://doi.org/10.4060/cd5968en, 2025.

Feng, S. J., Xu, W., Cheng, M. M., Ma, Y. X., Wu, L. B., Kang, J. H., Wang, K., Tang, A. H., Jeffrey L. C J., Fang, Y. T., Keith, G., Liu, X. J., Zhang F. S.: Overlooked Nonagricultural and Wintertime Agricultural NH3 Emissions in Quzhou County, North China Plain: Evidence from 15N-Stable Isotopes, Environ. Sci. Tech. Let., 9(2), 127-133, http://doi.org/10.1021/acs.estlett.1c00935, 2022.

Fleagle, R. G.: Atmospheric processes, Science, 140(3567), 653-654, http://doi.org/10.1126/science.140.3567.653.b, 1963.

Glotfelty, D. E., M. M. Leech, J. Jersey, and A. W. Taylor.: Volatilization and wind erosion of soil surface applied atrazine, simazine, alachlor, and toxaphene, Journal of agricultural and food chemistry, 37(2), 546-551, http://doi.org/10.1021/jf00086a059, 1989.

Gungormus, E., A. Sofuoglu, H. Celik, K. Gedik, M. D. Mulder, G. Lammel, S. C. Sofuoglu, E. Okten, T. Ugranli, and A. Birgul.: Selected persistent organic pollutants in ambient air in Turkey: Regional sources and controlling factors, Environ. Sci. Technol., 55(14), 9434-9443,

http://doi.org/10.1021/acs.est.0c06272, 2021.
Guo, L. P., Shi, S. P., Li, Y., M. Brüggemann, Zhao, M. Y., Mu, H. Y., D. M. Figueiredo, Wu, J. X. and Wang, K.: Gas-particle partitioning of pesticides in the atmosphere of the North China Plain [Dataset], Zenodo, https://doi.org/10.5281/zenodo.17641894, 2025.
Harner, T., and T. F. Bidleman.: Octanol− air partition coefficient for describing particle/gas partitioning of aromatic compounds in urban air, Environ. Sci. Technol., 32(10), 1494-1502, http://doi.org/10.1016/S1352-2310(97)00013-7, 1998.He, J. and R.: Balasubramanian. A study of gas/particle partitioning of SVOCs in the tropical atmosphere of Southeast Asia, Atmos. Environ., 43(29), 4375-4383, http://doi.org/10.1016/j.atmosenv.2009.03.055, 2009.
Hebei Provincial Bureau of Statistics. Hebei statistical yearbook 2024. China Statistics Press. 2024.
Hu, Y., Wu, S., Wu, C., Wei, Z., Ning, J. and D. She.: Risk assessment of airborne agricultural pesticide exposure in humans in rural China, Environ Geochem Health, 46(4), 117, http://doi.org/10.1007/s10653-024-01882-y, 2024.
Iakovides, M., K. Oikonomou, J. Sciare, and N. Mihalopoulos.: Evidence of stockpile contamination for legacy polychlorinated biphenyls and organochlorine pesticides in the urban environment of Cyprus (Eastern Mediterranean): influence of meteorology on air level variability and gas/particle partitioning based on equilibrium and steady-state models, J. Hazard. Mater., 439, 129544, http://doi.org/10.1016/j.jhazmat.2022.129544, 2022.
Jiang, L., Gao, W., Ma, X., Wang, Y., Wang, C., Li, Y., Yang, R., Fu, J., Shi, J., Zhang. Q. H., Wang, Y. W., Jiang, G. B.: Long-term investigation of the temporal trends and gas/particle partitioning of short- and medium-chain chlorinated paraffins in ambient air of King George Island, Antarctica, Environ. Sci. Technol., 55(1), 230-239, http://doi.org/10.1021/acs.est.0c05964, 2020.
Karla Solano Díaz, Clemens Ruepert, María Melania Ramírez Quesada, Jane A. Hoppin, Frank Wania, and Berna van Wendel de Joode.: Evaluation of passive air sampling for monitoring Current-Use Pesticide pollution near large-scale banana plantations in Costa Rica. Environ. Sci. Technol., 60 (4), 3384-3393, http://doi.org/10.1021/acs.est.5c11224, 2026.
Kaur, R., G. K. Mavi, S. Raghav, and I. Khan.: Pesticides classification and its impact on environment, Int. J. Curr. Microbiol. Appl. Sci, 8(3), 1889-1897, http://doi.org/10.20546/ijcmas.2019.803.224, 2019.
Li, Y., and M. Shiraiwa.: Timescales of secondary organic aerosols to reach equilibrium at various temperatures and relative humidities, Atmos. Chem. Phys., 19(9), 5959-5971, http://doi.org/10.5194/acp-19-5959-2019, 2019.
Li, Y. -F., Ma, W. -L., Yang, M.: Prediction of gas/particle partitioning of polybrominated diphenyl ethers (PBDEs) in global air: A theoretical study, Atmos. Chem. Phys., 15(4), 1669-1681, https://doi.org/10.5194/acp-15-1669-2015, 2015.
Lohmann, R., F. M. Jaward, L. Durham, J. L. Barber, W. Ockenden, K. C. Jones, R. Bruhn, S. Lakaschus, J. Dachs, and K. Booij.: Potential contamination of shipboard air samples by diffusive emissions of PCBs and other organic pollutants: Implications and solutions, Environ. Sci. Technol., 38(14), 3965-3970, http://doi.org/10.1021/es035005l, 2004.
Mayer, L., C. Degrendele, P. Šenk, J. Kohoutek, P. Přibylová, P. Kukučka, L. Melymuk, A. Durand, S. Ravier, A. Alastuey, A. R. Baker, U. Baltensperger, K. Baumann-Stanzer, T. Biermann, P. Bohlin-Nizzetto, D. Ceburnis, S. Conil, C. Couret, A. Degórska, E. Diapouli, S. Eckhardt, K. Eleftheriadis, G. L. Forster, K. Freier, F. Gheusi, M. I. Gini, H. Hellén, S. Henne, H. Herrmann, A. Holubová Šmejkalová, U. Hõrrak, C. Hüglin, H. Junninen, A. Kristensson, L. Langrene, J. Levula, M. Lothon,

E. Ludewig, U. Makkonen, J. Matejovičová, N. Mihalopoulos, V. Mináriková, W. Moche, S. M. Noe, N. Pérez, T. Petäjä, V. Pont, L. Poulain, E. Quivet, G. Ratz, T. Rehm, S. Reimann, I. Simmons, J. E. Sonke, M. Sorribas, R. Spoor, D. P. J. Swart, V. Vasilatou, H. Wortham, M. Yela, P. Zarmpas, C. Zellweger Fäsi, K. Tørseth, P. Laj, J. Klánová, and G. Lammel.: Widespread Pesticide Distribution in the European Atmosphere Questions their Degradability in Air, Environ. Sci. Technol., 58(7), 3342-3352, http://doi.org/10.1021/acs.est.3c08488, 2024.

McEachran Andrew, D., R. Blackwell Brett, J. D. Hanson, J. Wooten Kimberly, D. Mayer Gregory, B. Cox Stephen, and N. Smith Philip.: Antibiotics, Bacteria, and Antibiotic Resistance Genes: Aerial Transport from Cattle Feed Yards via Particulate Matter, Environ. Health Perspect., 123(4), 337-343, http://doi.org/10.1289/ehp.1408555, 2015.

Ministry of Agriculture and Rural Affairs of the People's Republic of China.: Ministry of Agriculture, Ministry of Industry and Information Technology, Ministry of Environmental Protection Announcement No. 1157, edited, http://www.moa.gov.cn/nybgb/2009/dsanq/201806/t20180606_6151221.htm, 2009.

Mu, H. Y. Zhang, J. C. Yang, X. M., Wang, K., Xu, W., Zhang, H. Y., Liu, X. J., C. J. Ritsema, V. Geissen.: Pesticide screening and health risk assessment of residential dust in a rural region of the North China Plain, Chemosphere, 303, 2, https://doi.org/10.1016/j.chemosphere.2022.135115, 2022.

Ngo, M., K. Pinkerton, S. Freeland, M. Geller, W. Ham, S. Cliff, L. Hopkins, M. Kleeman, U. Kodavanti, and E. Meharg.: Airborne particles in the San Joaquin Valley may affect human health, California Agriculture, 64(1), 12-16, http://doi.org/10.3733/ca.v064n01p12, 2010.

Pankow, J. F.: Review and comparative analysis of the theories on partitioning between the gas and aerosol particulate phases in the atmosphere, Atmospheric Environment , 21(11), 2275-2283, http://doi.org/10.1016/0004-6981(87)90363-5, 1987.

Qiao, L. N., Zhang, Z. F., Liu, L. Y., Song, W. W., Ma, W. L., Zhu, N. Z. and Li, Y. F.: Measurement and modeling the gas/particle partitioning of organochlorine pesticides (OCPs) in atmosphere at low temperatures, Sci. Total Environ, 667, 318-324, http://doi.org/10.1016/j.scitotenv.2019.02.347, 2019.

Sanlı, G. E., and Y. Tasdemir.: Seasonal variations of organochlorine pesticides (OCPs) in air samples during day and night periods in Bursa, Turkey, Atmospheric Pollution Research, 11(12), 2142-2153, http://doi.org/10.1016/j.apr.2020.06.010, 2020.

Scheyer, A., S. Morville, P. Mirabel, and M. Millet.: Gas/particle partitioning of lindane and current-used pesticides and their relationship with temperature in urban and rural air in Alsace region (east of France), Atmos. Environ., 42(33), 7695-7705, http://doi.org/10.1016/j.atmosenv.2008.05.029, 2008.

Skevas T, Stefanou SE, Oude Lansink A. Pesticide use, environmental spillovers and efficiency: A DEA risk-adjusted efficiency approach applied to Dutch arable farming. Eur J Oper Res, 237(2), 658-664, https://doi.org/10.1016/j.ejor.2014.01.046, 2014

Socorro, J., A. Durand, B. Temime-Roussel, S. Gligorovski, H. Wortham, and E. Quivet.: The persistence of pesticides in atmospheric particulate phase: An emerging air quality issue, Sci. Rep., 6(1), 33456, http://doi.org/10.1038/srep33456, 2016.

Sun, H., Chen, H., Yao, L., Chen, J. P., Zhu, Z. H., Wei, Y. Q., Ding, X., Chen, J. M.. Sources and health risks of PM2.5-bound polychlorinated biphenyls (PCBs) and organochlorine pesticides (OCPs) in a North China rural area, J. Environ. Sci., 95, 240-247, https://doi.org/10.1016/j.jes.2020.03.051, 2020.

Tian L, Li J, Zhao S, Tang J, Li J, Guo H, et al. DDT, Chlordane, and Hexachlorobenzene in the Air of the Pearl River Delta Revisited: A Tale of Source, History, and Monsoon. Environ. Sci. Technol., 55(14): 9740-9749, http://doi.org/10.1021/acs.est.1c01045, 2021.

Tudi, M., Li, H. R., Li, H. Y., Wang, L., Lyu, J., Yang, L. S., Tong, S. M., Q. J. Yu, H. D. Ruan, and A. Atabila, D. T. Phung, R. Sadler, and D. Connell.: Exposure routes and health risks associated with pesticide application, Toxics, 10(6), 335, http://doi.org/10.3390/toxics10060335, 2022.

Turusov, V., V. Rakitsky, and L. Tomatis.: Dichlorodiphenyltrichloroethane (DDT): ubiquity, persistence, and risks, Environ. Health Perspect.,110(2), 125-128, http://doi.org/10.1289/ehp.02110125, 2002.

Van den Berg, F., R. Kubiak, W. G. Benjey, M. S. Majewski, S. R. Yates, G. L. Reeves, J. H. Smelt, and A. M. A. van der Linden.: Emission of Pesticides into the Air, Water, Air, and Soil Pollution, 115(1), 195-218, http://doi.org/10.1023/A:1005234329622, 1999.

Wang, D. Q., Jia, S. M., Yang, P. F., Zhu, F. J. and Ma, W. L.: Size-resolved gas-particle partitioning of polycyclic aromatic hydrocarbons in a large temperature range of 50°C, J. Hazard. Mater., 479, 135607, http://doi.org/https://doi.org/10.1016/j.jhazmat.2024.135607, 2024.

Wang, S. R., A. Salamova, and M. Venier.: Occurrence, Spatial, and Seasonal Variations, and Gas–Particle Partitioning of Atmospheric Current-Use Pesticides (CUPs) in the Great Lakes Basin, Environ. Sci. Technol., 55(6), 3539-3548, http://doi.org/10.1021/acs.est.0c06470, 2021.

Woodrow, J. E., K. A. Gibson, and J. N. Seiber.: Pesticides and related toxicants in the atmosphere, Reviews of Environmental Contamination and Toxicology, 247, 147-196, http://doi.org/10.1007/398_2018_19, 2019.

Yu, B. G., Liu, Y.-M., Chen, X.-X., Cao, W.-Q., Ding, T. B. and Zou, C. Q.: Foliar Zinc Application to Wheat May Lessen the Zinc Deficiency Burden in Rural Quzhou, China, Frontiers in Nutrition, 8, http://doi.org/10.3389/fnut.2021.697817, 2021.

Yusà, V., C. Coscollà, W. Mellouki, A. Pastor, and M. De La Guardia.: Sampling and analysis of pesticides in ambient air, Journal of Chromatography A, 1216(15), 2972-2983, http://doi.org/10.1016/j.chroma.2009.02.019, 2009.

Zhao, M. Y., Wu, J. X., D. M. Figueiredo, Zhang, Y., Zou, Z. Y., Cao, Y. X., Li, J. J., Chen, X., Shi, S. P., Wei, Z. Y., Li, J. D., Zhang, H. Y., Zhao, E. C., V. Geissen, C. J. Ritsema, Liu, X. J., Han, J. J. and Wang, K.: Spatial-temporal distribution and potential risk of pesticides in ambient air in the North China Plain, Environ. Int., 182, 108342, http://doi.org/10.1016/j.envint.2023.108342, 2023.

Zhou, Y., Guo, J. Y., Wang, Z. K., Zhang, B. Y., Sun, Z., Yun, X. and Zhang, J. B.: Levels and inhalation health risk of neonicotinoid insecticides in fine particulate matter (PM2.5) in urban and rural areas of China, Environ. Int., 142, 105822, http://doi.org/10.1016/j.envint.2020.105822, 2020.

Zhu, F. J., Ma, W.-L., Liu, L.Y., Zhang, Z. F., Song, W. W., Hu, P. T., Li, W. L., Qiao, L. N. and Fan, H. Z.: Temporal trends of atmospheric PAHs: Implications for the gas-particle partition, Atmos. Environ., 261, 118595, http://doi.org/https://doi.org/10.1016/j.atmosenv.2021.118595, 2021.